Pergamon

Chaos, Solitons & Fractals, Vol. 8, No. 9, pp. 1431–1448, 1997

0960-0779/97 $17.00 + 0.00

PII: S0960-0779(96)00169-5

Adaptive Strategies for Recognition, Control and Synchronization of Chaos

S. BOCCALETTI, A. FARINI and F. T. ARECCHI†

Istituto Nazionale di Ottica, I-50125 Firenze, Italy

Abstract—We review a series of adaptive algorithms which recognize chaos, stabilize the unstable periodic orbits embedded in a chaotic attractor and synchronize two identical chaotic systems starting from different initial conditions, by exploiting the information of the local contraction or expansion rates of a chaotic system. This adaptive strategy is applied to the chaotic Lorenz, the three- and four-dimensional Rössler and the delayed Mackey–Glass systems. © 1997 Elsevier Science Ltd

1. INTRODUCTION

Recent papers [1–3] have introduced different adaptive strategies for chaos recognition, control and synchronization.

There are two different methods for inspecting a (possibly continuous) dynamical system: the standard one which consists of selecting a regularly spaced series of observation times and plotting the evolution of the corresponding coordinates in some state space. Based upon this geometrical series of data, one decides whether a signal is regular, chaotic or random.

An alternative approach, whenever the motion is confined within a finite region of space, consists of fixing a narrow observation window in the coordinate space and registering only data within that window. This way, the geometric positions are a clustered set, but the sequence of return times to the window is erratic if the dynamics is irregular. In more complex dynamics, with multi-branched attractors, as, for example, in the Lorenz case, the above argument fails in correspondence to sudden jumps from one branch to the other; indeed, if the window selects positions of one branch, the time sequence is affected by big holes whenever the flow jumps to other branches and hence the stroboscopic series provides only partial information on the chaotic motion.

In this report we describe the implementation of a stroboscopic inspection which overcomes the above difficulty, through an adaptive windowing controlled by the local variation (expansion or contraction) rates. In Section 2 we show how this procedure provides useful indicators for chaos recognition, even for systems displaying more than one positive Liapunov exponent. In Section 3 we apply this method to the control of the different unstable periodic orbits (UPO) embedded within the chaotic attractor (CA) and in Section 4 we combine adaptation with synchronization of a chaotic dynamics in order to warrant secure communication between a message sender and a receiver.

†Also at: Department of Physics, University of Firenze, I-50125 Firenze, Italy.

2. ADAPTIVE RECOGNITION OF CHAOS

Let us consider a dissipative dynamics $\dot{\mathbf{x}} = \mathbf{f}(\mathbf{x},\mu)$, where $\mathbf{x}$ is a D-dimensional vector and μ a set of control parameters, and start by setting μ beyond the first chaotic bifurcation in order to have an unstable periodic orbit of period $\bar{\tau}$.

In this section, we aim at recognizing the unperturbed features of this dynamics. For this purpose, based upon the information provided by the local variation rates, we adjust the next observation time interval (OTI) shorter or longer than $\bar{\tau}$, in order to minimize the variation in width of the window including the two points at the extreme of the interval.

We consider an observer who is 'blind' to the main coordinate position x_i ($i = 1,...,D$) and interested only in its variation

$$\delta x_i(t_{n+1}) = x_i(t_{n+1}) - x_i(t_n), \tag{1}$$

where $t_{n+1} - t_n = \tau_n$ is the nth adjustable interval, to be specified. In order to assign τ_{n+1} we consider the local variation rate

$$\lambda_i(t_{n+1}) = \frac{1}{\tau_n} \ln \left| \frac{\delta x_i(t_{n+1})}{\delta x_i(t_n)} \right|. \tag{2}$$

Here τ_{n+1} is the minimum of all $\tau_{n+1}^{(i)}$ corresponding to the different i, defined by the rule

$$\tau_{n+1}^{(i)} = \tau_n^{(i)}(1 - \tanh(g\lambda_i(t_{n+1}))). \tag{3}$$

Equation (3) arises from the following considerations. To obtain a sequence of geometrically regular δx_i, we contract (expand) the OTI when the actual value of δx_i is bigger (smaller) than the previously observed one. The hyperbolic tangent function maps the whole range of $g\lambda_i$ into the interval $(-1, +1)$. The constant g, strictly positive, is chosen in such a way as to forbid $\tau_n^{(i)}$ from going to zero. It may be taken as an *a priori* sensitivity. A more sensible assignment would consist of looking at the unbiased dynamical evolution for a while and then taking a g value smaller than the reciprocal of the maximal λ recorded in that time span. Choosing a fixed g is like adjusting the connectivities of a neural network by a preliminary learning session, while adjusting g upon the information accumulated over a given number of previous time steps corresponds to considering g as a kind of long-term-memory, as opposed to the short-term-memory represented by the sequence of τ_n [4].

We thus obtain a sequence of observation times starting from t_0

$$t_0, t_1 = t_0 + \bar{\tau}, t_2 = t_1 + \tau_1,..., t_{n+1} = t_n + \tau_n,... \tag{4}$$

corresponding to which the variations of $\delta x_i(t_n)$ can be reduced below a preassigned value.

The observations performed at these times provide a 'regularized' window and the time sequence (4) now includes the chaotic information which was in the original geometric sequence $\mathbf{x}(t)$. The same strategy has been implemented in a neural network approach with applications to real time Monte Carlo calculations as well as to real time recognition of particle tracks in high energy experiments [5].

Here we show how the above algorithm can be applied to many chaotic situations such as the Lorenz model (Lo) [6], the three- and four-dimensional Rössler model (respectively called Ro3 [7] and Ro4 [8]) and the Mackey–Glass delay equation (MG) [9].

For the (x,y) variables of Lo ($\sigma = 10$, $b = 8/3$, $r = 60$) and Ro3 ($a = 0.2$, $b = 0.2$, $c = 9.0$), we evaluate the actual values $x(t)$, $y(t)$ and the observed values $x(t_n)$, $y(t_n)$ according to our

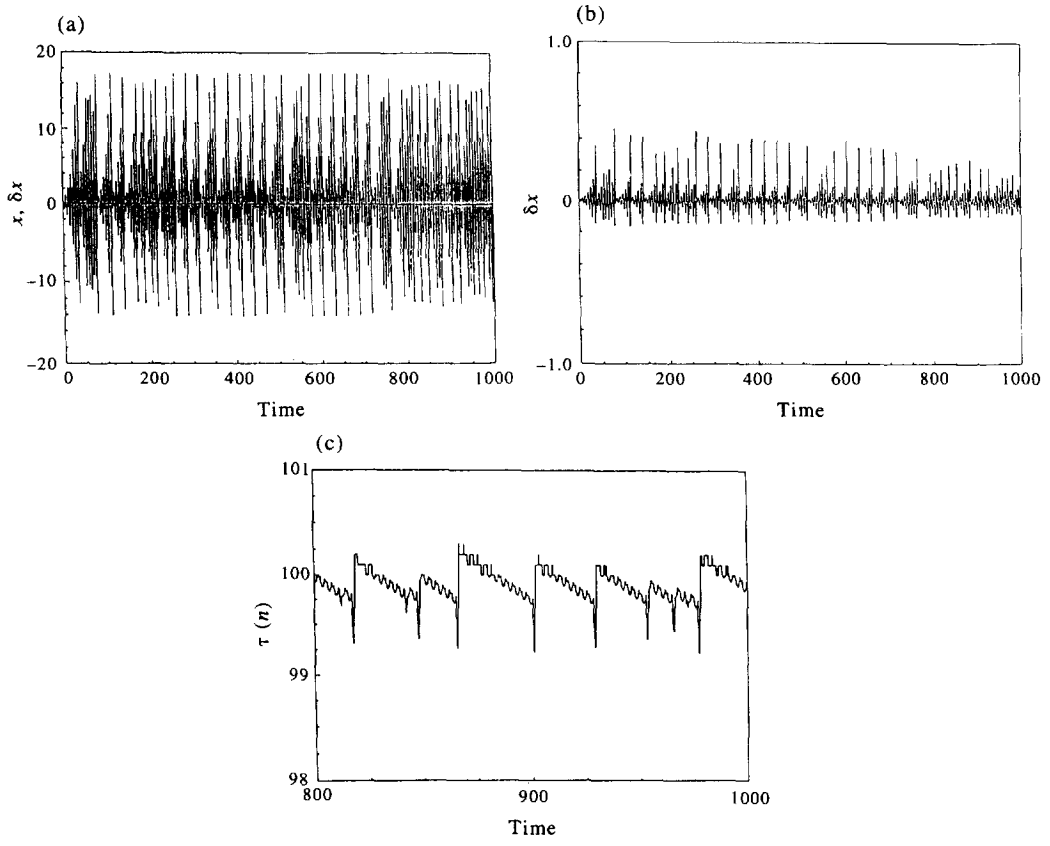

Fig. 1. (From Ref. [1]) Adaptive windowing around a chaotic attractor. (a) $x(t)$ and $\delta x(t_{n+1}) = x(t_n + \tau_n) - x(t_n)$ (central line) for chaotic Ro3 ($a = 0.2$, $b = 0.2$, $c = 9.0$) dynamics; $\bar{\tau} = 0.01$, $g = 0.00015$. (b) δx on expanded vertical scale. (c) Observer time interval τ_n vs the absolute time t (vertical scale magnified by 10^4).

regularization procedure and compare these values with the differences δx, δy. As an example, we report x and δx for Ro3 in Fig. 1. The magnified vertical scale of Fig. 1(b) shows that the window is confined within a range two orders of magnitude smaller than the variation range of $x(t)$.

The OTI sequence [Fig. 1(c)] contains the relevant information on the dynamics, and we can characterize chaos as follows. Since in equation (3) $|g\lambda_i| < 1$, then two successive τ_n must be strongly correlated. As a result, even though the set of τ_n may be spread over a rather wide support [as shown in Fig. 1(c)], the return map τ_{n+1} versus τ_n must cluster along the diagonal. Any appreciable deviation from the diagonal denotes the presence of uncorrelated noise. This is shown in Fig. 2 where we plot the return map of the τ_n for Ro4 and for Ro4 with 1% noise.

The above method provides a criterion to forecast whether a string of data corresponds to a deterministic or stochastic phenomenon. A very stringent test for this inductive problem is represented by MG

$$\dot{x} = -0.1x(t) + \frac{0.2x(t-T)}{1 + x(t-T)^{10}}. \tag{5}$$

With $T = 100$ it corresponds to a ~7.5 dimensional chaotic dynamics [10].

Using the embedding technique, we consider the time series for MG, for a pure white noise with r.m.s. fluctuations as MG, and for a random phase time series having the same

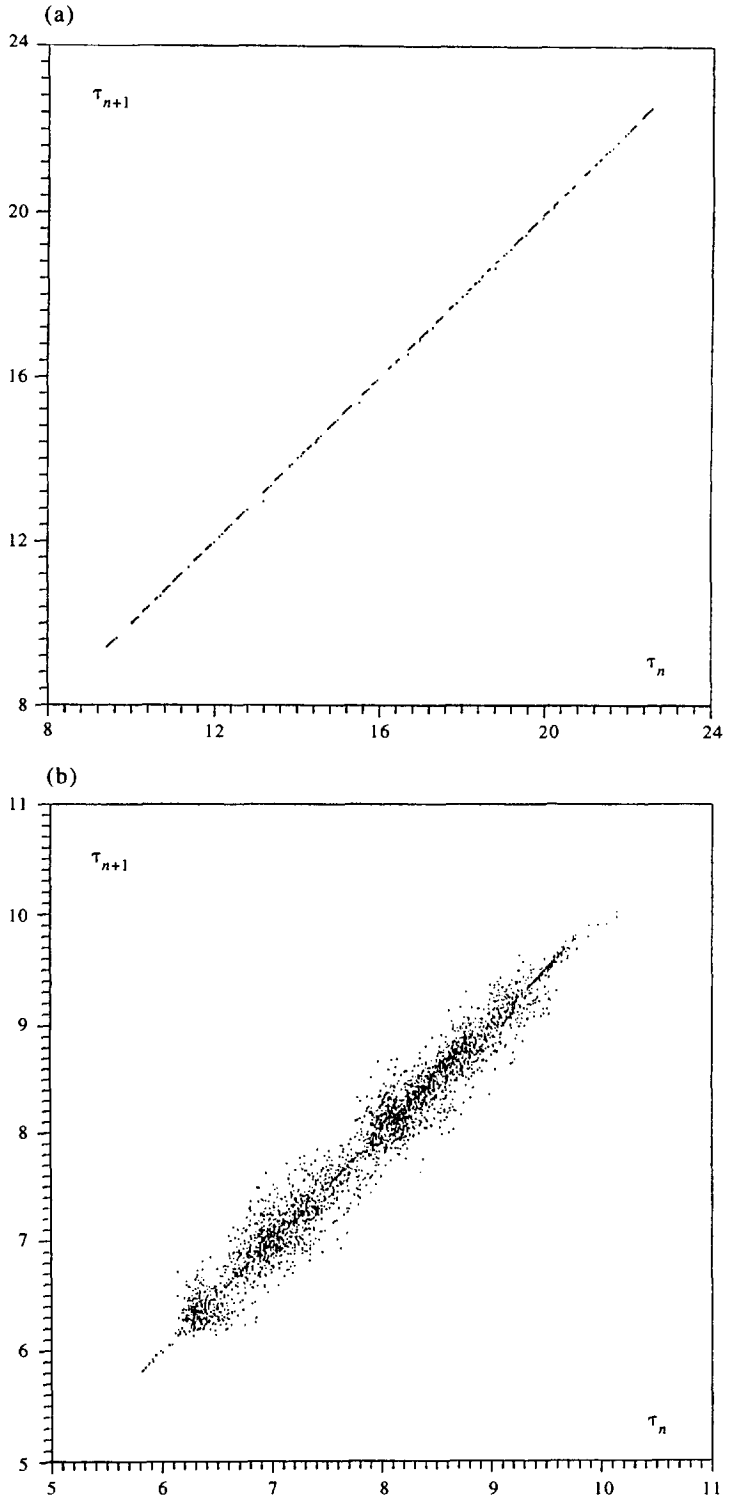

Fig. 2. (From Ref. [1]) Return maps τ_{n+1} vs τ_n for (a) Ro4 and (b) Ro4 with an additional 1% white noise. Initial conditions: $x(0) = -20$, $y(0) = z(0) = 0$, $w(0) = 15$. $g = 0.000048$.

spectral power as MG (surrogate) [11]. A stringent condition is provided by the volume variation rate $\prod_{i=1}^{m}\lambda_i(n)$ in the m-dimensional embedding space of the window around each point at $t_n = n$. For a deterministic series, as we increase the embedding dimension m beyond $D+1$, where D is the effective dimension of the chaotic attractor, the extra added dimensions remain unfilled. On the contrary, a noise signal tends to fill all available dimensions. Thus the new indicator

$$\beta = \frac{1}{N}\sum_{n}\prod_{i=1}^{m}\lambda_i(n) \tag{6}$$

provides a very sensitive discrimination between determinism and noise.

Its heuristic meaning emerges from the following considerations. Expanding equation (2) to first order and referring to the unit time step $\tau_n = 1$, we can write $\lambda_i(t_{n+1}) = (\delta x_i(t_{n+1}) - \delta x_i(t_n))/\delta x_i(t_n)$. We now evaluate the variation over the unit time of the volume $V_n = \prod_{i=1}^{m}\delta x_i(t_n)$ made by all m measured variations at time t_n. The relative variation rate $r_n = (V_{n+1} - V_n)/V_n$ is given by

$$r_n = \sum_i \lambda_i + \sum_{i\neq j}\lambda_i\lambda_j + \ldots + \prod_i \lambda_i. \tag{7}$$

Summing up over all directions of the embedding space, we introduce the directional averages

$$\langle\lambda\rangle = \frac{1}{m}\sum_i \lambda_i, \quad \langle\lambda^2\rangle = \frac{2}{m(m-1)}\sum_{i\neq j}\lambda_i\lambda_j, \text{ etc.} \tag{8}$$

and the above equation (7) reads as

$$r_n = m\langle\lambda\rangle + \frac{m(m-1)}{2}\langle\lambda^2\rangle + \ldots\langle\lambda^m\rangle. \tag{9}$$

As we further sum over all n up to N, the twisting along the chaotic trajectory makes all directions statistically equivalent, thus in $\Sigma_n r_n$ we can replace $<\lambda^k>$ by $<\lambda>^k$ for $2 \leq k \leq m$. In the case of stochastic noise, since variations over successive time steps are uncorrelated, $\delta x(t_{n+1}) - \delta x(t_n) \simeq \delta x(t_n)$ and $<\lambda>$ is close to 1, so that $<\lambda>^m = O(1)$. Instead of a deterministic dynamics two successive steps are strongly correlated, hence $<\lambda> < 1$, and the last term of equation (9) yields the most sensitive test, since it decays as $\exp(-m\log(1/\langle\lambda\rangle))$.

Based on these considerations, we take the sum over the N trajectory points of the last term of equation (9) as a suitable indicator, as displayed in equation (6).

In view of what has been said above, β scales as e^{-m} for a deterministic signal [aside a factor $O(1)$ in the exponent] whereas it scales as e^0 for noise. In the case of the surrogate of a deterministic system, one half of the total number of degrees of freedom (the phases of each Fourier component) scales like noise, while the other half (the amplitudes of each Fourier component) scales like the deterministic signal. As a result, we expect a global scaling law $e^{-0.5m}$.

Figure 3 shows the β plots versus m for MG and its surrogate as well as for white noise. The three plots have exponential fits $\exp(-Am)$ with $A = 1$, 0.5 and 0, respectively, for MG, surrogate and white noise.

Comparing our adaptive recognition with statistical methods based upon the assignment of a probability measure in phase-space, as counting the number of neighbors within a given distance from each phase-point [12] or the distribution of distances for closest neighbors [13], we easily realize that, for M data points, the number of computing operations scales as M in our case and as M^2 in statistical cases. Furthermore, to assure a good resolution in m

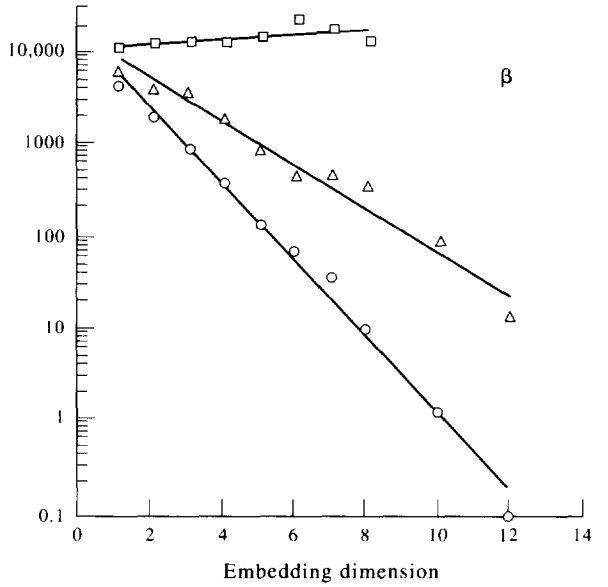

Fig. 3. (From Ref. 1) β plots vs embedding dimension m. Squares: white noise; triangles: surrogate of MG; circles: MG attractor. For all cases $g = 0.0048$. Solid lines are exponential fits e^{Am}, with $A = 0.039$ for white noise, $A = -0.526$ for the surrogate of MG and $A = -0.987$ for MG.

embedding dimensions, statistical methods require that M increase exponentially in m, whereas our adaptive strategy is based on variation rates along the coordinate axes and hence our M scales linearly with m. Similar comparative remarks also hold for recent tests for determinism [14], based on exploring the evolution of a neighborhood of close points.

3. ADAPTIVE CONTROL OF CHAOS

Controlling chaos consists of perturbing a chaotic system in order to stabilize a given unstable periodic orbit (UPO) embedded in the chaotic attractor (CA) [15].

The first control method proposed by Ott, Grebogi and Yorke (OGY) [16] consists of slight readjustment of a control parameter each time the trajectory crosses the Poincaré section (PS). Since a generic UPO is mapped on the PS by an ordered sequence of crossing points, OGY is able to stabilize such a sequence whenever the chaotic trajectory closely visits a neighborhood of one of the saddle PS points. It can happen that the time lapse for a natural passage of flow within the fixed neighborhood (hence the reason for switching on the control process) is very large. To minimize such a waiting time, a technique of targeting has also been introduced [17].

Another technique to constrain a nonlinear system $\mathbf{x}(t)$ following a prescribed goal dynamics $\mathbf{g}(t)$ has been introduced [18] based upon the addition to the equation of motion $d\mathbf{x}/dt = \mathbf{F}(\mathbf{x})$ of the term $\mathbf{U}(t)$ chosen in such a way that $|\mathbf{x}(t) - \mathbf{g}(t)| \to 0$ as $t \to \infty$. Reference [18] considers $\mathbf{U}(t) = (d\mathbf{g})/(dt) - \mathbf{F}(g(t))$. Even though the method provides robust solutions, in general the perturbation $\mathbf{U}$ to be done is of the same order of magnitude as the unperturbed dynamics $\mathbf{F}$.

In other papers the effects of periodic [19–20] and stochastic [21] perturbations is explored by producing dramatic changes in the dynamics, which, however, are quite difficult to predict and in general are not goal oriented.

A further method [22] has been proposed, based upon the continuous application of a delayed feedback term in order to force the dynamical evolution of the system toward the desired periodic dynamics whenever the system closely visits such a periodic behavior.

On the other hand, many experimental systems have been studied with the aim of establishing control over chaos.

Experimental chaos control and higher order periodic orbit stabilization have been successfully carried out in dealing with a thermal convection loop [23], a yttrium iron garnet oscillator [20], a diode resonator [24], an optical multimode chaotic solid-state laser [25], a Belouzov–Zabotinsky chemical reaction [26] and a CO_2 laser with modulation of losses [27]. In most cases, stabilization of UPOs was achieved by the technique of occasional proportional feedback (OPF) introduced in Ref. [24].

Even though a discrete hyperchaotic (with more than one positive Liapunov exponent) dynamics has been controlled [28] and targetted [29], extension of the above methods to continuous hyperchaotic dynamics is still an open question.

In this section we report on the application of the adaptive method, which intervenes with the adaptive time scale T_s intermediate between the short resolution time T_1 of continuous methods [22] and the long one T_2 corresponding to the delay between two successive PS crossings used in Ref. [16].

Let us consider a general dynamical dissipative system ruled by

$$\dot{\mathbf{x}} = \mathbf{G}(\mathbf{x}, \mu), \tag{10}$$

where $\mathbf{x}$ is a D-dimensional vector, $\mathbf{G}$ a nonlinear function and μ a set of control parameters chosen in such a way as to produce chaos. We have already discussed in the previous section [equations (1)–(3)] how adaptive observation can be performed, and how the obtained sequence of stroboscopic times t_0, $t_1 = t_0 + \tilde{\tau}$, $t_2 = t_1 + \tau_1$,..., $t_{n+1} = t_n + \tau_n$,... now contains the relevant information on the dynamics. Characterization and recognition of chaos can be done by the study of such a time sequence.

In the following, we will summarize the application of such a method to the Lo model and to the Ro4 model. The latter consists of a four-dimensional dynamical system described by the equations

$$\begin{aligned} \dot{x}_1 &= -x_2 - x_3 \\ \dot{x}_2 &= x_1 + 0.25x_2 + x_4 \\ \dot{x}_3 &= 3 + x_1 x_3 \\ \dot{x}_4 &= -0.5x_3 + 0.05x_4 \end{aligned} \tag{11}$$

For initial conditions $x_1(0) = -20$, $x_2(0) = x_3(0) = 0$, $x_4(0) = 15$, and for the values of control parameters displayed in the equations, equation (11) produces a hyperchaotic dynamics with two positive Liapunov exponents [8].

Since we are interested in stabilizing a periodic dynamics, we need to extract the periods of UPOs embedded within the CA. For this purpose, instead of considering the single step map (as in the previous section), we construct the maps τ_{n+k} versus τ_n, $k = 1,2,...$ and plot the r.m.s. η of the point distribution around the diagonal of such maps as functions of the step interval k. For chaotic dynamics, temporal selfcorrelation lasts only for a finite time, hence one should expect to obtain a monotonically increasing function. In fact, the chaotic dynamics brings the trajectory into the phase-space to shadow the neighborhoods of the different UPOs. As the trajectory gets close to a UPO of period T_j, the temporal selfcorrelation is rebuilt after T_j and the distribution of τ includes windows of correlated

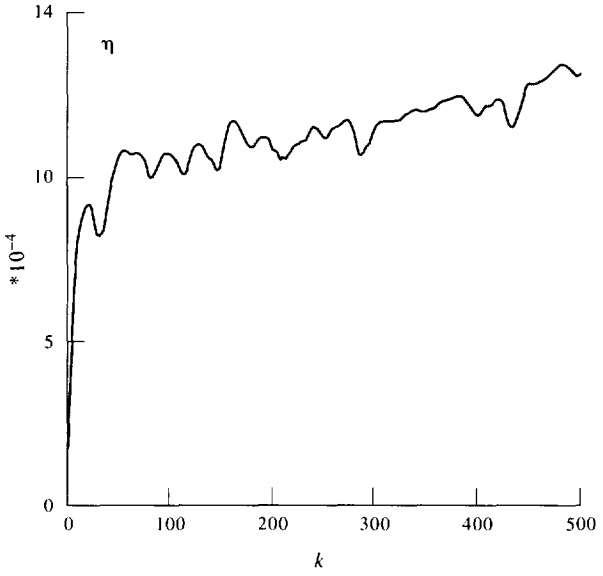

Fig. 4. (From Ref. [2]) η–κ plot for Ro4 attractor. Initial conditions and control parameters as in the text. The recognition task has been performed with $g = 0.01$. The vertical axis has to be multiplied by 10^{-4}.

values appearing as minima of η versus k around $k_j = T_j/\langle\tau\rangle$, $\langle\tau\rangle$ being the average of the τ distribution.

To give an example, in Fig. 4 we report the η–k plot for Ro4, from which one can extract the different UPO periods looking at the minima of the η curve. In fact, during the stroboscopic observation, the OTIs are changing, and a more rigorous determination of the period is provided by looking at a suitable cost function in the vicinity of the minima of the η curve.

Let us call $\tau_{\min}$ and $\tau_{\max}$, respectively, the minimum and the maximum τ values during the recognition task. It is evident that the period T_j of the jth UPO is such that

$$k_j\tau_{\min} \leq T_j \leq k_j\tau_{\max}$$

where k_j is the jth minimum of the η curve. Thus, introducing a cost function

$$C(\nu) = \sum_{n=1}^{N} \mathbf{x}(t_n) - \mathbf{x}(t_n - \nu), \tag{12}$$

where the sum runs over the N data recorded during the recognition task, and looking for the minimum of $C(\nu)$ with ν running from $k_j\tau_{\min}$ to $k_j\tau_{\max}$, one obtains the real period T_j of the jth UPO of the dynamics under study.

Figure 5 shows the cost function $C(\nu)$ for the eighth minimum of the η plot. $\nu = 54.64$ measures the value of the period-8 UPO of Ro4.

Once the periods $T_j (j = 1,2,...)$ of the UPOs have been measured, stabilization of each one can be achieved when the system naturally closely visits the phase space neighborhoods of that UPO. For a nonautonomous system it can happen that a period T corresponds to many degenerated UPOs. In this case, selection of the desired one can be provided by study of the topology of all UPOs corresponding to the same period and by switching on the control task when the system is shadowing the selected UPO. Some topological approaches to the UPO's detection are contained in Ref. [30].

The control procedure is done by use of the following modified algorithm. At each new

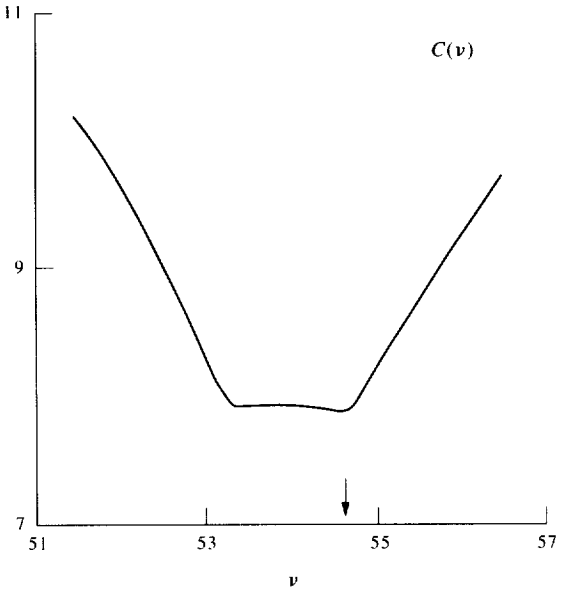

Fig. 5. (From Ref. [2]) Cost function $C(\nu)$ for the eighth k minimum of Fig. 4. $\nu = 54.64$ (indicated by the arrow) is the measurement of the period for one of the orbit 8s of Ro4.

observation time $t_{n+1} = t_n + \tau_n$ and for each component i of the dynamics, instead of equation (1), we evaluate the differences δ between actual and desired values:

$$\delta x_i(t_{n+1}) = x_i(t_{n+1}) - x_i(t_{n+1} - T_j), \tag{13}$$

and the local variation rates λ now read

$$\lambda_i(t_{n+1}) = \frac{1}{\tau_n} \log \left| \frac{x_i(t_{n+1}) - x_i(t_{n+1} - T_j)}{x_i(t_n) - x_i(t_n - T_j)} \right|. \tag{14}$$

Equations (2) and (3) and the choice of the minimum are kept for the updating process of τ. Defining $\mathbf{U}(t)$ as the vector with the ith component (constant over each observation time interval) given by

$$U_i(t_{n+1}) = \frac{1}{\tau_{n+1}} (x_i(t_{n+1} - T_j) - x_i(t_{n+1})), \tag{15}$$

we add such a vector to the evolution equation, which now reads

$$\frac{\mathrm{d}\mathbf{x}}{\mathrm{d}t} = \mathbf{G}(x, \mu) + \mathbf{U}(t). \tag{16}$$

Notice now that λs measure how the separation of the actual trajectory from the desired one evolves; indeed, a negative λ means that locally the true orbit is collapsing into the desired one and hence the actual dynamics is shadowing the desired UPO. On the contrary, a positive λ implies that the actual trajectory is locally diverging away from the desired one and control has to be performed in order to constrain the orbit to shadow the desired UPO.

As a consequence, contraction or expansion of τs now reflects the necessity to perturb the dynamics more or less often in order to stabilize the desired UPO, as well as fixing the weight of the correction to be done, which, once a given T_j has been chosen by the operator,

is selected by the same adaptive dynamics. Integrating equation (16) from t_{n+1} to t_{n+2}, since $\mathbf{U}(t)$ is constant over τ_{n+1}, yields the term $\mathbf{x}(t_{n+1} - T_j) - \mathbf{x}(t_{n+1})$ which exactly corrects for the previously observed chaotic deviation from the goal dynamics.

Once again, the introduced adaptive weighting procedure in equation (15) assures the effectiveness of the method (perturbation is larger or smaller whenever it has to be) as well as the fact that the additive term **U** is much smaller than the unperturbed dynamics **G**.

In Fig. 6 we show the control of period-8 of Ro4 and of period-5 of Lo. In the last case, a larger initial δ has been selected in order to highlight the shadowing process.

Finally, in Fig. 7 we report the perturbation $U_1(t)$ and the unperturbed dynamics G_1 for the Ro4 model during the control task of period-8, in order to show that the former is

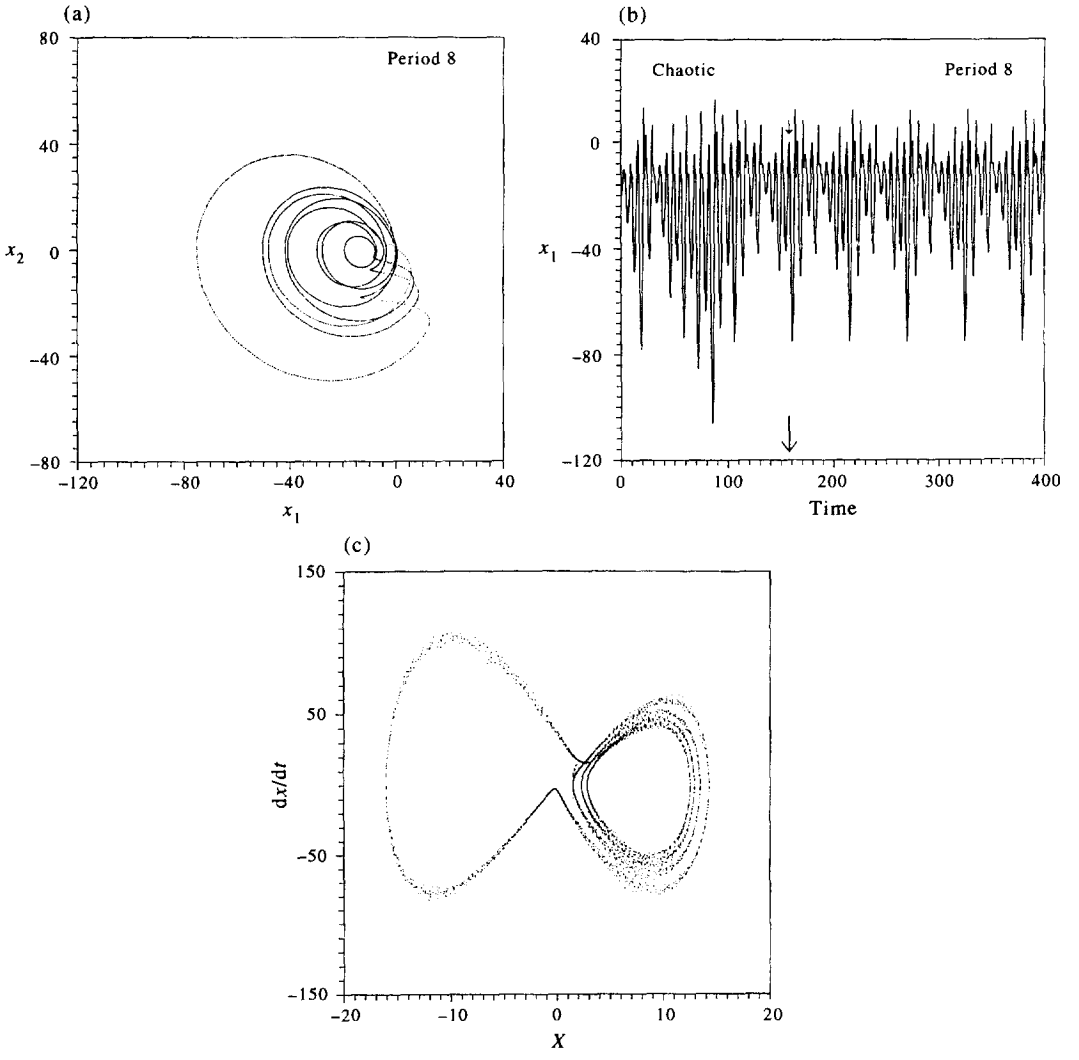

Fig. 6. (From Ref. [2]) (x_1,x_2) projection of the phase space portrait for the controlled period-8 of the Ro4 attractor. (a) The control task has been performed with period-8 extracted from Fig. 5 and $g = 10^{-5}$. (b) Time evolution of the first component x_1 of Ro4 before and after control. Arrows indicate the instance at which the control task begins. (c) $(x, \dot{x})$ representation for the period-5 of Lo ($\sigma = 10$, $b = 8/3$, $r = 25$). In this latter case the control task has been provided with period-5 measured by the minimum of the cost function ($T = 6.09$), $g = 10^{-5}$, but the control has been switched on when the distance between the true orbit and desired period was quite large in order to highlight the shadowing process.

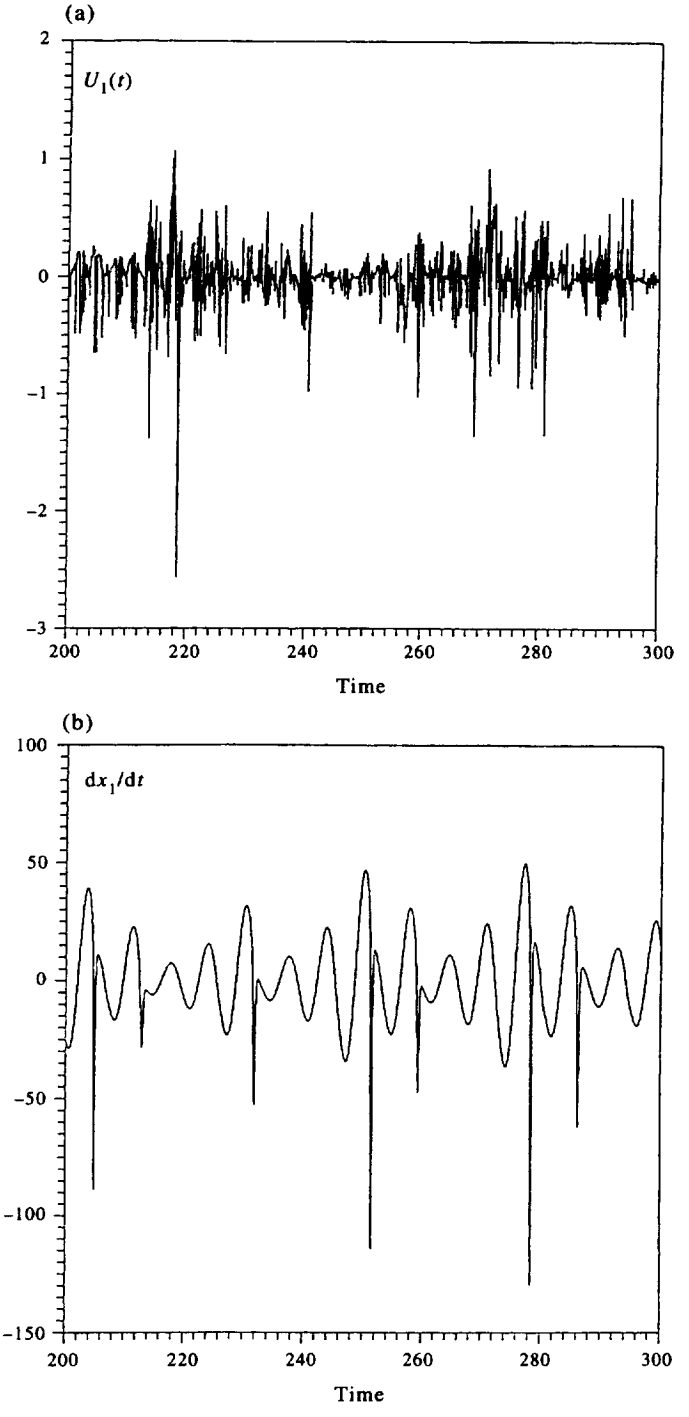

Fig. 7. (From Ref. [2]) (a) Temporal evolution of the first component of the additive controlling term U_1 during the control of period-8 of Ro4 and (b) temporal evolution of the uncontrolled $(dx_1)/(dt)$. The adaptive correction term is between two and three orders of magnitude smaller than the natural evolution of the dynamics. The same stipulation for the controlling task as mentioned in the caption of Fig. 6.

between two and three orders of magnitude smaller than the latter as expected by the above discussion.

As for time scales, notice that while in equation (13) differences δx_i are evaluated with respect to the goal dynamics (thus over the period T_j), in equation (14) all λs are evaluated over the adaptive τ, which, as discussed in Ref. [1], has to be much larger than the Runge–Kutta integration interval (about 100 times larger) but much smaller than the UPO period (as is evident from Fig. 4 where all k_js are much above unity). This way the method introduces a natural adaptation time scale intermediate between the minimum resolution time and time scale of the periodic orbits.

In summary, the method acts in two successive steps: an initial recognition task in which the periods of UPOs are extracted from the unperturbed dynamics and a second control task whereby one can constrain the system to a given periodic orbit. The second step can also be used for slaving a given dynamics $\mathbf{x}(t)$ to a goal dynamics $\mathbf{g}$ by simply redefining the differences in equation (13) as $\delta x_i(t_{n+1}) = x_i(t_{n+1}) - g_i(t_{n+1})$ and keeping equations (14)–(16) with the new δs for the updating τ process and for the controlling process.

The main difference between this method and OGY is that the adaptive technique does not act on the control parameters, and it needs neither calculation of the PS for the system under study, nor study of the local dynamics of the different UPOs on the PS.

Notice that the limit $g = 0$ of our algorithm recovers Ref. [22]. Choosing $g \neq 0$ implies two novel features. First, the adaptive nature of the forcing term [equation (15)], which is inversely proportional to the time intervals and hence is weighted by the information extracted from the dynamics itself. Second, while in Ref. [22] the control is readjusted at each computational time step, here interventions are done at the intermediate time scale, thus reducing the computational or experimental effort for the control task.

4. ADAPTIVE SYNCHRONIZATION OF CHAOS

The considerations developed in the previous sections can be successfully applied to the problem of synchronization of chaos. The idea of synchronizing two identical chaotic systems starting from different initial conditions was introduced by Pecora and Carrols (PC) [31]. It consists of linking the trajectory of one system to the same values as the other so that they remain in step with each other, through transmission of a signal. In Ref. [31], this process has been realized when the subLiapunov exponents of the subsystem to be synchronized are all negative.

On the other hand, the possibility of encoding a message within a chaotic dynamics [32] has been recently shown. This suggests the use of chaos synchronization to produce secure communication between a sender and a receiver. However, several problems arise in order to assure security in the communication. The main one is due to the fact that the sender must transmit at least one of the system variables to the receiver. As a result, a clever spy intercepting the communications can reconstruct the whole dynamics, hence decoding the message. To prevent interceptions, Cuomo and Hoppenheim [33] have proposed to use chaos to hide messages. This way, the transmitted signal is the sum of a chaotic signal and a given message which can be reconstructed by the receiver once it has been synchronized with the sender. However, Perez and Cerdeira [34] have shown that messages masked by low-dimensional chaotic processes, once intercepted, can sometimes be readily extracted. Attention has later been directed to the implementation of the PC idea to higher dimensional systems [35] where increased unpredictability may improve security in the communication. However, the possibility of decoding the system through the reconstruction of the signal is still not fully prevented.

Other problems rely on the limitations of the PC procedure to those subsystems which show negative subLiapunov exponents. Thus, any additive signal introduced to hide the real message should be an infinitesimal perturbation of the signal itself, with the same effect as the natural noise within the communication procedure.

Even though enrichment of the PC method has been done or alternative approaches to synchronization based on nonreplica subsystems have been proposed [36], the problem of security in the communications is not yet fully resolved.

In this section we review the application of the adaptive scheme for chaos synchronization whereby one can overcome the above difficulties and security in the communication is guaranteed against external interceptions. This scheme combines the PC idea with the adaptive algorithm reviewed above. Let us suppose we have a message sender (Alice) and a receiver (Bob) in the presence of a spy (James) ready to intercept and decode any communication between them. Alice consists of two identical chaotic systems

$$\dot{\mathbf{x}}_1 = \mathbf{f}(\mathbf{x}_1, \mu),$$

$$\dot{\mathbf{x}}_2 = \mathbf{f}(\mathbf{x}_2, \mu), \tag{17}$$

where μ is a set of control parameters chosen in such a way as to produce chaos, $\mathbf{x}_1$,$\mathbf{x}_2$ are two D-dimensional vectors ($D \geq 3$) and $\mathbf{f}$ is a nonlinear function. On the other hand, Bob consists of a third identical system

$$\dot{\mathbf{x}}_3 = \mathbf{f}(\mathbf{x}_3, \mu). \tag{18}$$

The three systems start from different initial conditions, thus producing unsynchronized dynamics. In the following, the three systems will be represented by the Lo system. Then the vectors $\mathbf{x}_j \equiv (x_j, y_j, z_j)$, $(j = 1,2,3)$ obey the equations:

$$\dot{x}_j = \sigma(y_j - x_j),$$

$$\dot{y}_j = r x_j - y_j - x_j z_j,$$

$$\dot{z}_j = -b z_j + x_j y_j. \tag{19}$$

We suppose that the message Alice must transmit to Bob be encoded in the variable $x_1(t)$. The scheme for the communication is represented in Fig. 8.

The first step is to produce synchronization between $\mathbf{x}_2$ and $\mathbf{x}_3$. Bob sends the variable $y_3(t)$ to Alice which is replaced in the equations for x_2 and z_2. Synchronization is assured by the fact that the subLiapunov exponents for the subsystem (x_2,z_2) are both negative [31] (for $\sigma = 10$, $b = 8/3$ and $r = 60$ they are -2.67 and -9.99, respectively).

Then Alice knows the whole actual dynamical state of Bob and consequently can transmit the perturbation $U(t)$ to Bob to be applied to the x_3 equation in order to synchronize the system $\mathbf{x}_3$ to $\mathbf{x}_1$. Alice makes use of the adaptive method to slave the system $\mathbf{x}_3$ to the goal dynamics $\mathbf{x}_1$. At any of Alice's observation times $t_{n+1} = t_n + \tau_n$, Alice defines the difference between current and target dynamics

$$\delta_{n+1} = x_2(t_{n+1}) - x_1(t_{n+1}), \tag{20}$$

and replaces the new definition of δ into equations (13)–(16). The perturbation $U(t)$ is now given by

$$U(t) = \frac{K}{\tau_{n+1}}(x_1(t) - x_2(t)). \tag{21}$$

To demonstrate the effectiveness of the proposed scheme, Fig. 9 reports the temporal

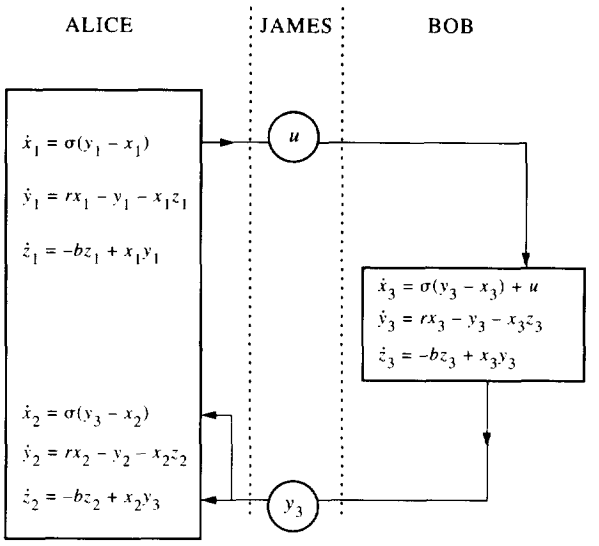

Fig. 8. (From Ref. [3]) The scheme for adaptive synchronization. Bob sends the variable y_3 to Alice to synchronize $\mathbf{x}_2$ and $\mathbf{x}_3$. Alice sends the adaptive correction $U(t)$ to Bob to be added to the evolution equation for x_3. James can intercept both $U(t)$ and y_3.

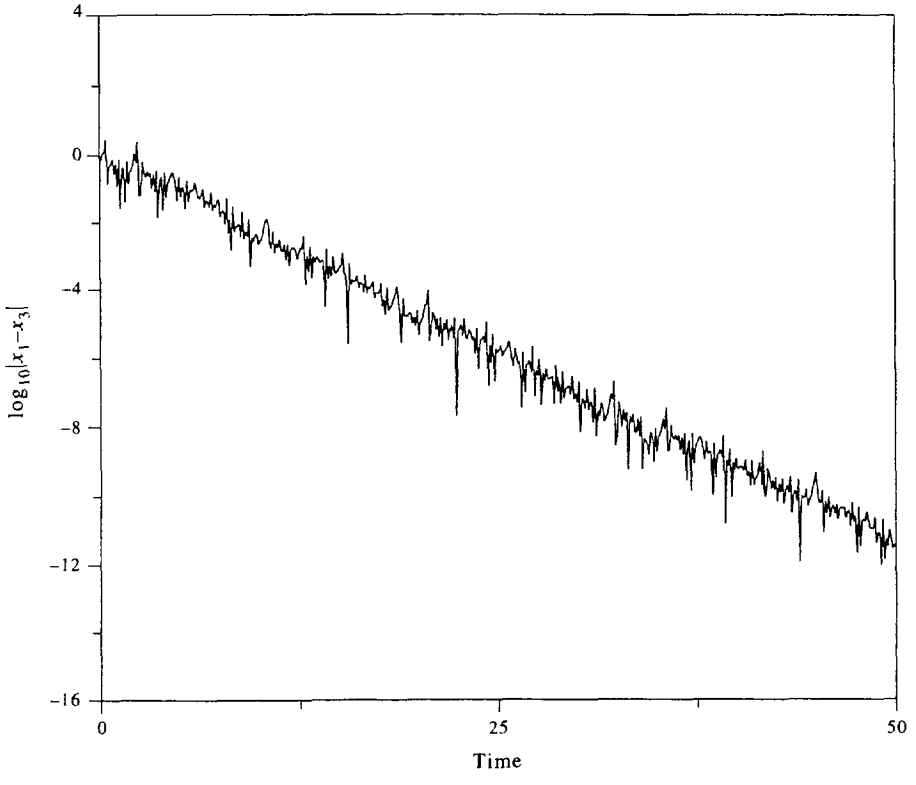

Fig. 9. (From Ref. [3]) Temporal evolution of the quantity $\log_{10}(|x_1 - x_3|)$ measuring the synchronization between $\mathbf{x}_1$ and $\mathbf{x}_3$, thus indicating how accurate Bob is at receiving and decoding the message sent by Alice. $\sigma = 10$, $b = 8/3$, $r = 60$, $\tau_0 = 0.01$, $g = 0.011$, $K = 0.1$.

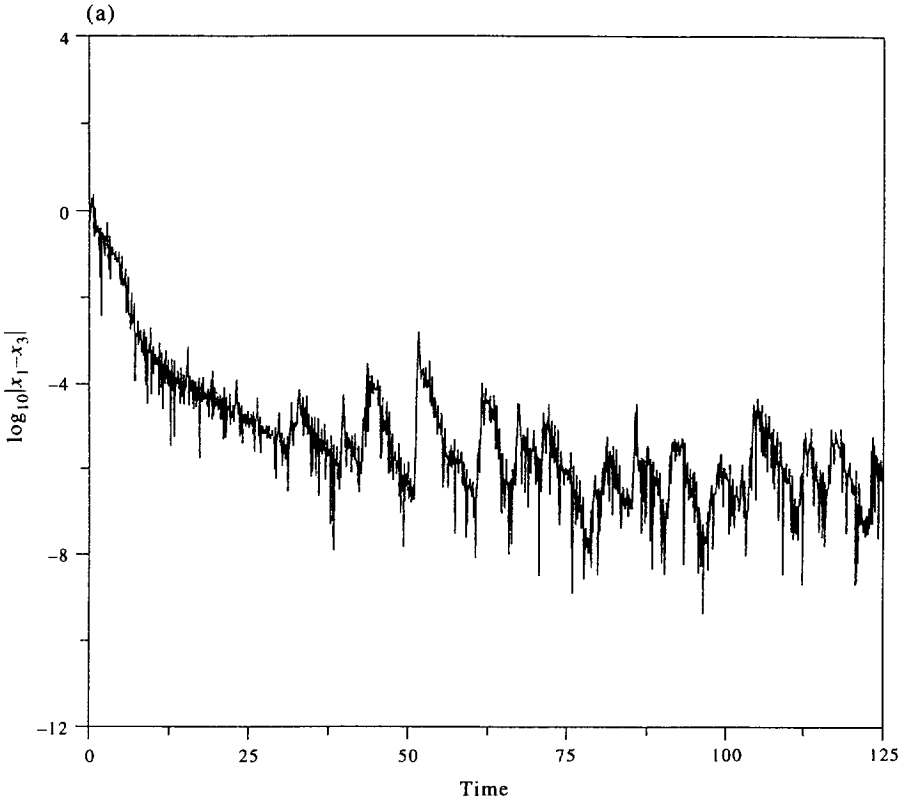

Fig. 10. *Caption overleaf.*

behavior of $\Delta x = |x_1 - x_3|$ which measures the synchronization between Alice and Bob for $\sigma = 10$, $b = 8/3$ and $r = 60$. Similar results also hold for $|y_1 - y_3|$ and $|z_1 - z_3|$, thus indicating that the systems $\mathbf{x}_1$ and $\mathbf{x}_3$ are globally synchronized. As a consequence, any message encoded within x_1 is easily received and decoded by Bob.

Let us now discuss the problem of security. James intercepts the two communication signals $U(t)$ and $y_3(t)$. No information on x_1 can be retrieved from $U(t)$ since $U(t)$ vanishes as soon as Alice and Bob reach synchronization, and the weighting factor K/τ_{n+1} is not decided *a priori*, but is continuously changed by the same dynamics (no fixed rule is available for James to decode the signal). One may speculate that, from the knowledge of y_3, James can reconstruct the whole CA corresponding to $\mathbf{x}_3$, hence the messages when $\mathbf{x}_3$ and $\mathbf{x}_1$ become synchronized.

To prevent this, once Alice and Bob have previously agreed on a given accuracy θ for the reception of the message, each time such an accuracy has been reached (Alice can test this since she has full information on the dynamical state of Bob), Bob stops sending y_3 for a given time lag T_0. In the meantime, the two systems $\mathbf{x}_2$ and $\mathbf{x}_3$ evolve separately. After T_0 Bob again starts sending y_3 to Alice. If T_0 exceeds the decorrelation time $\tilde{\tau}$ of the system (the reciprocal of the maximum Liapunov exponent Λ), then the effective signal sent by Bob to Alice results in the collection of uncorrelated temporal subsequences, and no reconstruction of $\mathbf{x}_3$ is possible by James in this case.

The procedure relies on the robustness of the synchronizing method. In Fig. 10 we report the results for $T_0 = 1$ and $\theta = 10^{-5}$ (notice that in our case $\Lambda \simeq 1.41$, hence $T_0 > \tilde{\tau} \simeq 0.71$). Our scheme is able to maintain the stipulated accuracy [Fig. 10(a)] even in the case in which the signal sent by Bob to Alice is affected by large holes [Fig. 10(b)] which prevent possible

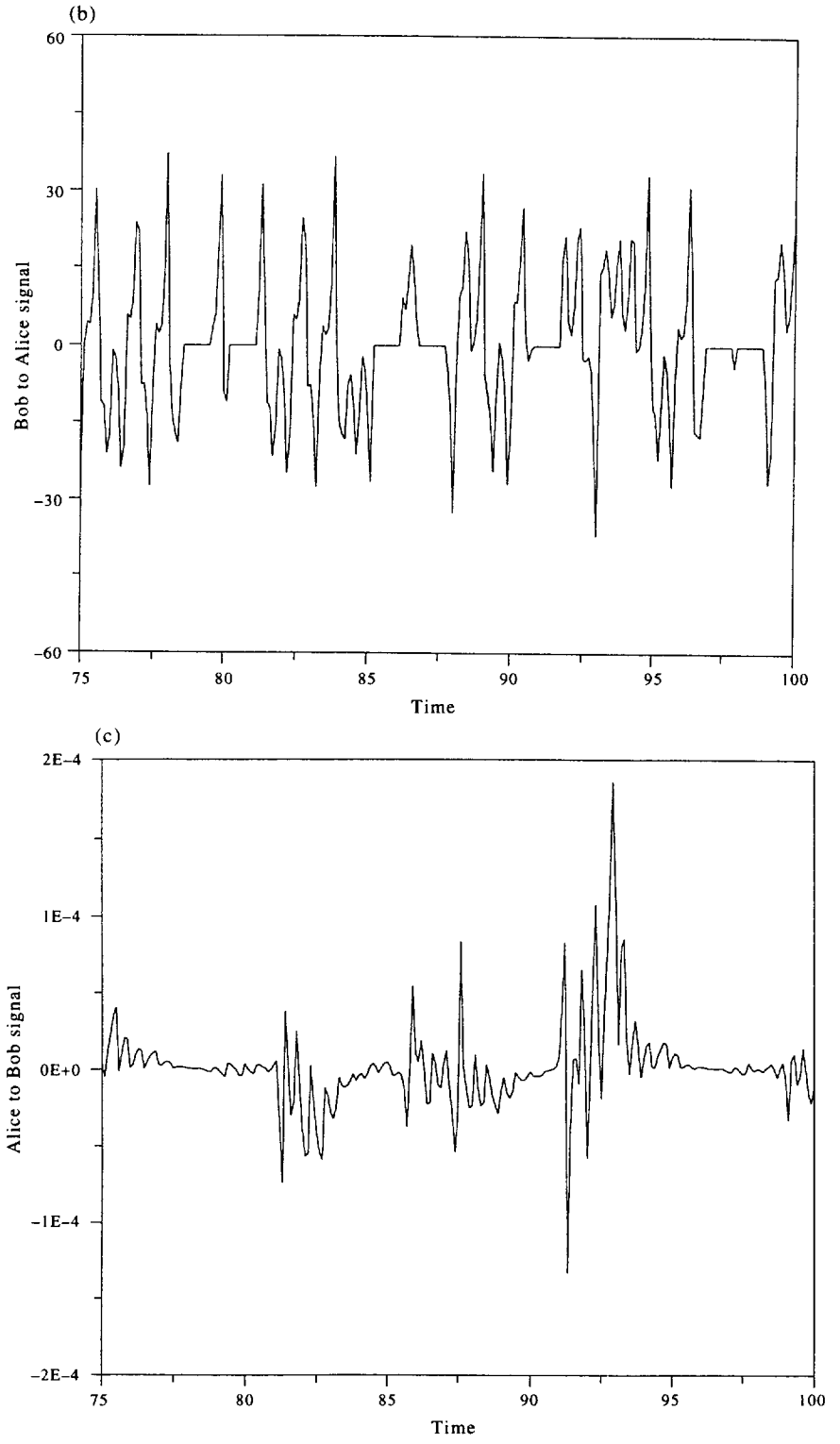

Fig. 10. (From Ref. [3]) (a) Temporal evolution of $\log_{10}(|x_1 - x_3|)$ for $\theta = 10^{-5}$ and $T_0 = 1 > (1/\Lambda) \simeq 0.71$. The stipulated accuracy in the transmission is preserved in time even though: (b) the synchronization signal Bob sends to Alice is affected by large holes which prevent any reconstruction of the message and (c) the controlling signal $U(t)$ is kept within a range negligible with respect to the dynamics. Other parameters are as in Fig. 9.

external reconstructions of $\mathbf{x}_3(t)$. Finally, Fig. 10(c) shows the controlling signal which remains confined within a range negligible with respect to the x_1 dynamics (x_1 variations from -28 to 28).

REFERENCES

1. Arecchi, F. T., Basti, G., Boccaletti, S. and Perrone, A. L., Adaptive recognition of a chaotic dynamics. *Europhys. Lett.*, 1994, **26,** 327; Arecchi, F. T., Basti, G., Boccaletti, S. and Perrone, A. L., Adaptive recognition of chaos. *Int. J. Bifurcation and Chaos*, 1994, **4,** 1275.
2. Boccaletti, S. and Arecchi, F. T., Adaptive control of chaos. *Europhys. Lett.*, 1995, **31,** 127; Boccaletti, S. and Arecchi, F. T., Adaptive recognition and control of chaos. *Physica*, 1996, **D96**, 9.
3. Boccaletti, S., Farini, A. and Arecchi, F. T., Adaptive synchronization of chaos for secure communication. Submitted to *Phys. Rev. Lett.*
4. Grossberg, S., Nonlinear neural networks: principles. *Mech. Architect. Neural Nets*, 1988, **1,** 17.
5. Basti, G. and Perrone, A. L., A theorem of computational effectiveness for a mutual redefinition of numbers and processes. *Proc. Int. Symp. of Information Physics (ISKIT '92)*, Kyushu Institute of Technology, 1992, p. 122.
6. Lorenz, E. N., Deterministic nonperiodic flow. *J. Atmos. Sci.*, 1963, **20,** 130.
7. Rössler, O. E., An equation for continuous chaos. *Phys. Lett.*, 1976, **57A,** 397.
8. Rössler, O. E., An equation for hyperchaos. *Phys. Lett.*, 1979, **71A,** 155.
9. Mackey, M. C. and Glass, L., Oscillation and chaos in physiological control systems. *Science*, 1977, **197,** 287.
10. Farmer, J. D., Chaotic attractors of an infinite-dimensional dynamical system. *Physica*, 1982, **D4,** 366; Grassberger, P. and Procaccia, I., Measuring the strangeness of strange attractors. *Physica*, 1983, **D9,** 189.
11. Theiler, J., Galdrikian, J., Longtin, A., Eubank, S. and Farmer, J. D., In *Nonlinear Modeling and Forecasting*, eds M. Casdagli and S. Eubank. Addison–Wesley, Reading, MA, 1992.
12. Grassberger, P. and Procaccia, I., Characterization of strange attractors. *Phys. Rev. Lett.*, 1983, **50,** 346.
13. Badii, R. and Politi, A., Hausdorff dimension and uniformity factor of strange attractors. *Phys. Rev. Lett.*, 1984, **52,** 1661.
14. Kaplan, D. T. and Glass, L., Direct test for determinism in a time series. *Phys. Rev. Lett.*, 1992, **68,** 427; Wayland, R., Bromley, D., Pickett, D. and Passamante, A., Recognizing determinism in a time series. *Phys. Rev. Lett.*, 1993, **70,** 580.
15. Auerbach, D., Cvitanovic, P., Eckmann, J.-P., Gunaratne, G. and Procaccia, I., Exploring chaotic motion through periodic orbits. *Phys. Rev. Lett.*, 1987, **58,** 2387.
16. Ott, E., Grebogi, C. and Yorke, J. A., Controlling chaos. *Phys. Rev. Lett.*, 1990, **64,** 1196.
17. Shinbrot, T., Grebogi, C., Ott, E. and Yorke, J. A. Using small perturbations to control chaos. *Nature*, 1993, **363,** 411.
18. Plapp, B. B. and Huebler, A. W., Nonlinear resonances and suppression of chaos in the rf-biased Josephson junction. *Phys. Rev. Lett.*, 1990, **65,** 2302; Jackson, E. A. and Huebler, A. W., Periodic entrainment of chaotic logistic map dynamics. *Physica*, 1990, **D44,** 407; Jackson, E. A., Controls of dynamic flows with attractors. *Phys. Rev.*, 1991, **A44,** 4839.
19. Lima, R. and Pettini, M., Suppression of chaos by resonant parametric perturbations. *Phys. Rev.*, 1990, **A41,** 726; Braiman, Y. and Goldhirsch, I., Taming chaotic dynamics with weak periodic perturbations. *Phys. Rev. Lett.*, 1991, **66,** 2545.
20. Azevedo, A. and Rezende, S. M., Controlling chaos in spin-wave instabilities. *Phys. Rev. Lett.*, 1991, **66,** 1342.
21. Fahy, S. and Hamann, D. R., Transition from chaotic to nonchaotic behavior in randomly driven systems. *Phys. Rev. Lett.*, 1992, **69,** 761.
22. Pyragas, K., Continuous control of chaos by self-controlling feedback. *Phys. Lett.*, 1992, **A170,** 421.
23. Singer, J., Wang, Y.-Z. and Bau, H. H., Controlling a chaotic system. *Phys. Rev. Lett.*, 1991, **66,** 1123.
24. Hunt, E. R., Stabilizing high-period orbits in a chaotic system: the diode resonator. *Phys. Rev. Lett.*, 1991, **67,** 1953.
25. Roy, R., Murphy, T. W. Jr, Maier, T. D., Gills, Z. and Hunt, E. R., Dynamical control of a chaotic laser: experimental stabilization of a globally coupled system. *Phys. Rev. Lett.*, 1992, **68,** 1259.
26. Peng, B., Petrov, V. and Showalter, K., Controlling chemical chaos. *J. Phys. Chem.*, 1991, **95,** 4957; Petrov, V., Gaspar, V., Masere, J. and Showalter, K., Controlling chaos in the Belousov–Zhabotinsky reaction, *Nature*, 1993, **361,** 240.
27. Meucci, R., Gadomski, W., Ciofini, M. and Arecchi, F. T., Experimental control of chaos by means of weak parametric perturbations. *Phys. Rev.*, 1994, **E49,** R2528.
28. Romeiras, F. J., Grebogi, C., Ott, E. and Dayawansa, W. P., Controlling chaotic dynamical systems. *Physica*, 1992, **D58,** 165.
29. Kostelich, E. J., Grebogi, C., Ott, E. and Yorke, J. A., Higher-dimensional targeting. *Phys. Rev.*, 1993, **E47,** 305.
30. Cvitanovic, P., Gunaratne, G. H. and Procaccia, I., Topological and metric properties of Hénon-type strange attractors. *Phys. Rev.*, 1988, **A38,** 1503; Gunaratne, G. H., Linsay, P. S. and Vinson, M. J., Chaos beyond onset: a comparison of theory and experiment. *Phys. Rev. Lett.*, 1989, **63,** 1; Mindlin, G. B., Hou, X.-J., Solari, H. G., Gilmore, R. and Tufillaro, N. B., Classification of strange attractors by integers. *Phys. Rev. Lett.*, 1990, **64,** 2350; Tufillaro, N. B., Solari, H. G. and Gilmore, R., Relative rotation rates: fingerprints for strange attractors. *Phys. Rev.*, 1990, **A41,** R5717.

31. Pecora, L. M. and Carrols, T. L., Synchronization in chaotic systems. *Phys. Rev. Lett.*, 1990, **64,** 821.
32. Hayes, S., Grebogi, C., Ott, E. and Mark, A., Experimental control of chaos for communication. *Phys. Rev. Lett.*, 1994, **73,** 1781.
33. Cuomo, K. M. and Oppenheim, A. V., Circuit implementation of synchronized chaos with application to communications. *Phys. Rev. Lett.*, 1993, **71,** 65.
34. Perez, G. and Cerdeira, H. A., Extracting messages masked by chaos. *Phys. Rev. Lett.*, 1995, **74,** 1970.
35. Peng, J. H., Ding, E. J., Ding, M. and Yang, W., Synchronizing hyperchaos with a scalar transmitted signal. *Phys. Rev. Lett.*, 1996, **76,** 904.
36. Ding, M. and Ott, E., Enhancing synchronism of chaotic system. *Phys. Rev.*, 1994, **E49,** R945.